AIP Journal of Applied Physics

Raman spectra and electron-phonon coupling in disordered graphene with gate-tunable doping

Isaac Childres, Luis A. Jauregui, and Yong P. Chen

Citation: Journal of Applied Physics **116**, 233101 (2014); doi: 10.1063/1.4903959
View online: http://dx.doi.org/10.1063/1.4903959
View Table of Contents: http://scitation.aip.org/content/aip/journal/jap/116/23?ver=pdfcov
Published by the AIP Publishing

Articles you may be interested in
Nitrogen doping of chemical vapor deposition grown graphene on 4H-SiC (0001)
J. Appl. Phys. **115**, 233504 (2014); 10.1063/1.4884015

Gate tunable graphene-silicon Ohmic/Schottky contacts
Appl. Phys. Lett. **101**, 223113 (2012); 10.1063/1.4768921

Spectroscopic investigation of nitrogen doped graphene
Appl. Phys. Lett. **101**, 123108 (2012); 10.1063/1.4752736

Plasmons in electrostatically doped graphene
Appl. Phys. Lett. **100**, 201105 (2012); 10.1063/1.4714688

Top-gate dielectric induced doping and scattering of charge carriers in epitaxial graphene
Appl. Phys. Lett. **99**, 013103 (2011); 10.1063/1.3607284

[This article is copyrighted as indicated in the article. Reuse of AIP content is subject to the terms at: http://scitation.aip.org/termsconditions. Downloaded to] IP: 128.210.68.204 On: Tue, 23 Dec 2014 22:27:15

JOURNAL OF APPLIED PHYSICS 116, 233101 (2014)

Raman spectra and electron-phonon coupling in disordered graphene with gate-tunable doping

Isaac Childres,[1,2,a)] Luis A. Jauregui,[2,3] and Yong P. Chen[1,2,3]
[1]Department of Physics, Purdue University, West Lafayette, Indiana 47907, USA
[2]Birck Nanotechnology Center, Purdue University, West Lafayette, Indiana 47907, USA
[3]School of Electrical and Computer Engineering, Purdue University, West Lafayette, Indiana 47907, USA

(Received 3 September 2014; accepted 28 November 2014; published online 15 December 2014)

We report a Raman spectroscopy study of graphene field-effect transistors with a controlled amount of defects introduced in graphene by exposure to electron-beam irradiation. Raman spectra are taken at $T = 8$ K over a range of back gate voltages (V_g) for various irradiation dosages (R_e). We study effects in the Raman spectra due to V_g-induced doping and artificially created disorder at various R_e. With moderate disorder (irradiation), the Raman G peak with respect to the graphene carrier density (n_{FE}) exhibits a minimum in peak frequency and a maximum in peak width near the charge-neutral point (CNP). These trends are similar to those seen in previous works on pristine graphene and have been attributed to a reduction of electron-phonon coupling strength (D) and removal of the Kohn anomaly as the Fermi level moves away from the CNP. We also observe a maximum in I_{2D}/I_G and weak maximum in I_D/I_G near the CNP. All the observed dependences of Raman parameters on n_{FE} weaken at stronger disorder (higher R_e), implying that disorder causes a reduction of D as well. Our findings are valuable for understanding Raman spectra and electron-phonon physics in doped and disordered graphene. © *2014 AIP Publishing LLC*.
[http://dx.doi.org/10.1063/1.4903959]

INTRODUCTION

Graphene has received much attention in the scientific community because of its distinct properties and potentials in nanoelectronic applications.[1,2] Raman spectroscopy,[3–5] which identifies vibrational modes using only laser excitation, is a powerful, non-invasive method to measure many important characteristics of graphene,[6] such as layer number, defect density, and carrier concentration.

In graphene, the Stokes phonon energy shift of laser excitation creates two main peaks in the Raman spectrum. The G peak ($\sim$1580 cm^{-1}) is the primary in-plane vibrational mode, caused by the E_{2g} phonon at the Γ point. The other major peak in graphene is 2D ($\sim$2690 cm^{-1}), which is created by a process of double scattering of A_{1g} phonons with an electron-hole pair between K to K′.[4]

In graphene, the K and Γ points of the Brillouin zone cause anomalous phonon dispersion due to rapidly changing electron screening of atomic vibrations at these points. This results in Kohn anomalies,[7] which soften phonons at wavevector $q \sim 2k_F$.[8] Doping in graphene, which shifts the Fermi level ($E_F \propto k_F$) away from the Dirac point, moves the Kohn anomaly (located at $2k_F$) away from $q = 0$. This causes a stiffening of the $q = 0$ G peak, increasing its phonon energy.[8,9] Increased doping also sharpens Raman peaks by reducing electron-phonon interactions through the blockage of decay channels from phonons into electron-hole pairs.[8,10] In addition, increased carrier doping in graphene has also been shown to decrease the intensity of the 2D peak.[11] By examining the widths, frequencies, and intensities of the G and 2D peaks in a graphene sample, one can gain information about its layer number, doping, and electron-phonon coupling strength (D).

Another well-studied peak in the Raman spectrum of graphene is the D peak ($\sim$1350 cm^{-1}), which is not activated in pristine graphene because of crystal symmetries. In order for the D peak to occur, a charge carrier must be excited and inelastically scattered by a phonon, then elastically scattered by a lattice defect or grain boundary to recombine.[12] Raman spectroscopy is one of the most widely used methods of defect characterization due to the strong dependence of graphene's Raman D peak on disorder. Disorder in graphene not only activates the D peak, which is caused by scattering from K to K′ (intervalley), but also gives rise to the D′ peak ($\sim$1620 cm^{-1}), caused by scattering from K to K (intravalley), and D + D′ ($\sim$2940 cm^{-1}), a combination scattering peak.[12] As has been previously reported, one can use the ratio of Raman peak intensities (I_D/I_G) to characterize the level of disorder in graphene.[13–20] As disorder in graphene increases, I_D/I_G displays 2 different behaviors: a regime of "low defect density," where I_D/I_G will increase with increased disorder as increasing defect density creates more elastic scattering; and a regime of "high defect density," where I_D/I_G will decrease with increased disorder as an increasing defect density results in a more amorphous carbon structure, attenuating all Raman peaks.[12]

There are very few studies, however, examining the effect of graphene carrier density (n_{FE}) on the Raman peaks in *disordered* graphene. Such a study will be important for gaining a more complete understanding of phonons and electron-phonon coupling in disordered graphene. In this work, we directly investigate the dependence of graphene's

[a)]Author to whom correspondence should be addressed. Electronic mail: ichildre@purdue.edu

 © 2014 AIP Publishing LLC

[This article is copyrighted as indicated in the article. Reuse of AIP content is subject to the terms at: http://scitation.aip.org/termsconditions. Downloaded to] IP: 128.210.68.204 On: Tue, 23 Dec 2014 22:27:15

Raman characteristics on both n_{FE} and the level of disorder in a graphene sample with disorder created by electron-beam irradiation. We are then able to extract an electron-phonon coupling strength as a function of disorder and show that this coupling strength weakens with increasing irradiation. These results demonstrate the importance of considering a graphene sample's disorder level and carrier density when characterizing it with Raman spectroscopy.

METHODS

Our graphene samples are fabricated using a similar method as in our previous publications.[16,17] We perform micromechanical exfoliation[2] of highly ordered pyrolytic graphite (HOPG, "ZYA" grade, Momentive Performance Materials) onto a p-doped Si wafer with 300 nm of SiO_2. Single-layer graphene flakes, typically around 100 μm^2 in size, are identified using color contrast with an optical microscope[21] and then confirmed with Raman spectroscopy.[12] Graphene field-effect devices are then fabricated using electron-beam lithography. The electrical contacts (5 nm Cr/35 nm Au) are fabricated by electron-beam evaporation.

The graphene sample is then placed in a scanning electron microscope (SEM), and a 25 μm by 25 μm area is continuously scanned by the electron beam to create disorder, as in our previous work.[16] The beam's kinetic energy is 30 keV, and the beam current is tuned so that the exposure takes 60 s of scanning. For instance, if the target irradiation dosage were 300 e^-/nm^2, a current of 0.4 nA would be used. In addition, the same sample is irradiated multiple times to reach a total accumulated dosage (R_e). For instance, after measuring the device at $R_e = 300$ e^-/nm^2, it is irradiated with a further 700 e^-/nm^2 (0.933 nA for 60 s) to arrive at $R_e = 1000$ e^-/nm^2. We note that the efficacy for the electron

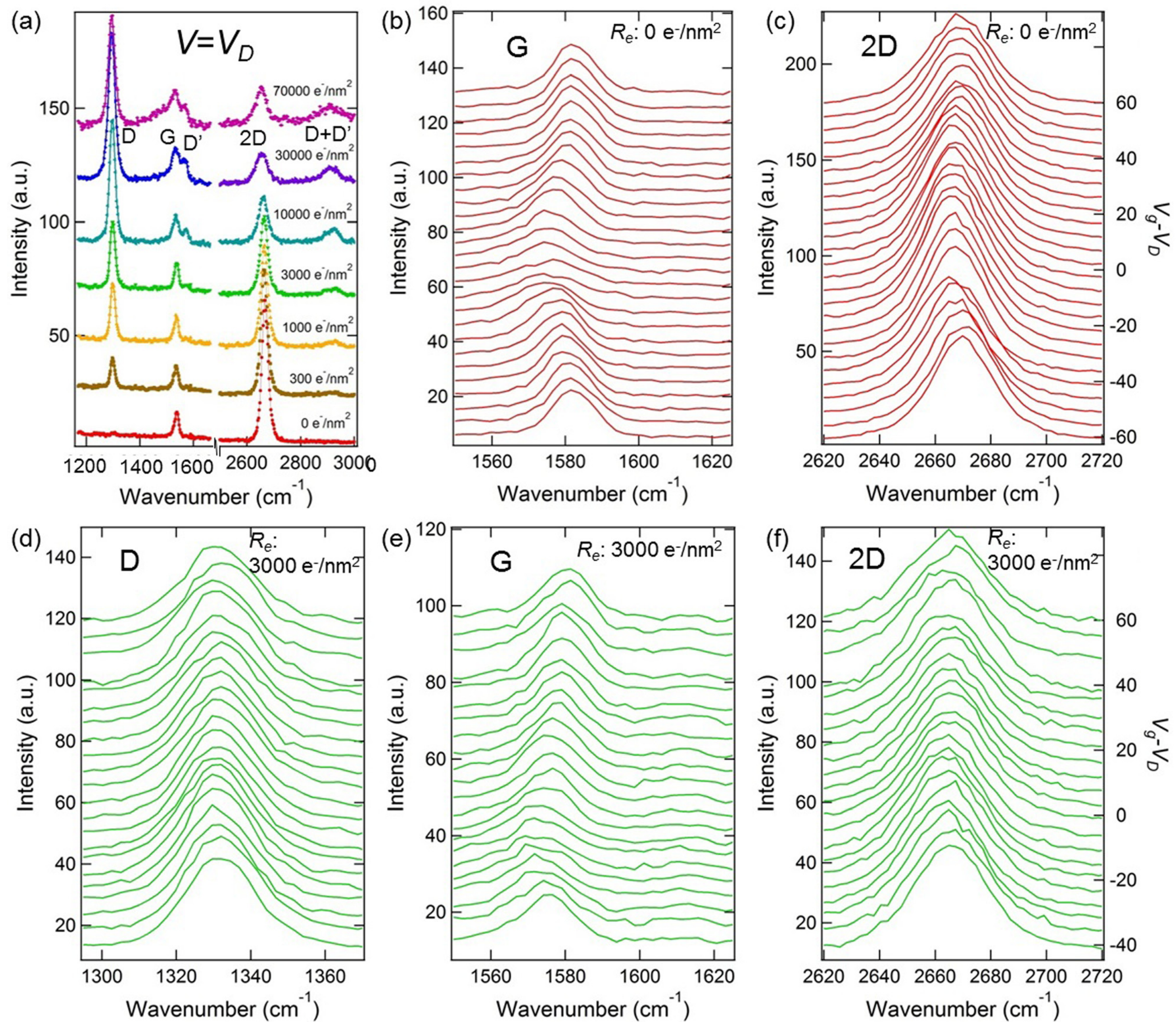

FIG. 1. (a) Raman spectra (measured with a 532 nm excitation laser) of graphene at its charge-neutral point (V_D) for different dosages (R_e) of irradiation by a 30 keV electron beam. Representative Raman peaks are labeled in the full spectrum for $R_e = 30\,000$ e^-/nm^2. (b) and (c) The G and 2D peaks, respectively, for unirradiated graphene at a range of back gate voltages (V_g, plotted on the right axis of (c) relative to V_D). (d)–(f) Raman spectra of the D, G, and 2D peaks, respectively, at different V_g (shown on the right axis of (f)) for the same graphene sample with an irradiation dosage $R_e = 3000$ e^-/nm^2. The spectra of all plots have been offset vertically for clarity.

[This article is copyrighted as indicated in the article. Reuse of AIP content is subject to the terms at: http://scitation.aip.org/termsconditions. Downloaded to] IP: 128.210.68.204 On: Tue, 23 Dec 2014 22:27:15

beam to create defects in graphene can vary for different experiments and R_e is related to, but does not provide a quantitative measurement of the defect length (L_D). All data shown in this paper are from a single graphene device and were taken over the course of a few days, though we have measured similar behaviors in several other samples.

The energy required to produce a ballistic ejection of an atom from a carbon lattice is ~86 keV,[22] three times larger than the 30 keV energy of the electrons used in this study, so vacancy defects can be excluded as a mechanism of disorder. We believe the defects caused by electron-beam irradiation to be "glide" and "shuffle" dislocations,[23] as discussed in previous reports.[14,20] We expect increased irradiation accumulation would increase the density of these dislocations.

After each successive exposure, the graphene device is removed from the SEM and transferred to a microscopy cryostat (Cryo Industries RC 102-CM) with electrical connections and an optical window and then brought to a temperature of ~8 K and a vacuum pressure of $\sim 10^{-5}$ mTorr. Field effect measurements (resistance versus back gate, V_g) are performed to determine capacitively induced n_{FE} of the graphene using

$$n_{FE} = \frac{\varepsilon_0 \varepsilon (V_g - V_D)}{te}, \tag{1}$$

where ε_0 and ε are the permittivities of free space and SiO_2, respectively, t is the thickness of the SiO_2 substrate, e is the electron charge, and V_D is the back gate voltage corresponding to the charge neutral point (CNP).

We note that the electron-beam irradiation process changes the carrier density of the device mainly by generating a positive bias from holes trapped at the SiO_2/Si after electron-hole pairs are excited by incoming irradiation.[16] Before every measurement, we measure the voltage of the CNP to ensure the accuracy of our n_{FE} value.

Raman spectroscopy is performed using a confocal microscope system (Horiba Xplora) with an excitation laser of 532 nm at a power of 0.1 mW incident on graphene, with each spectrum presented as an average of 3 measurements of 20 s each. Using a 100× objective, the Raman laser spot size is smaller than 1 μm^2. We characterize each Raman peak (G, D, and 2D) by a Lorentzian fit

$$f(\omega) = \frac{1}{2\pi} \cdot \frac{I\Gamma}{(\omega - \omega_0)^2 + \left(\frac{\Gamma}{2}\right)^2}, \tag{2}$$

where ω_0 is the peak position, Γ is the full width at half max (FWHM), and I is the integrated intensity of the full peak curve. Near 1600 cm^{-1} in the Raman spectrum for a disordered sample there is an overlap of the G and D′ peaks, and we fit those peaks together using a double-Lorentzian fit.

DATA

Fig. 1 shows the Raman spectra for our graphene device at various R_e and n_{FE}. Fig. 1(a) shows representative spectra from $R_e = 0$ e$^-$/nm^2 to 70 000 e$^-$/nm^2 at the graphene device's CNP. The spectra progression from unirradiated to highly irradiated ($R_e = 30\,000$ e$^-$/nm^2) shows a trend of decreasing 2D intensity (I_{2D}) and increasing D, D′, and D+D′ intensities with irradiation. Figs. 1(b) and 1(c) show the spectra near the G and 2D peaks, respectively, for the unirradiated device at different V_g ranging from −60 V to +60 V away from the CNP. This progression of spectra shows a minimum in the G peak frequency (ω_G) and a maximum in the G peak width (Γ_G) near the device's CNP. This is consistent with previous studies of G peak dependence on n_{FE} for pristine graphene (with no appreciable disorder to have an observable D peak).[8–11] Figs. 1(d)–1(f) show the spectra near the D, G, and 2D peaks, respectively, for the same device after moderate irradiation ($R_e = 3000$ e$^-$/nm^2)

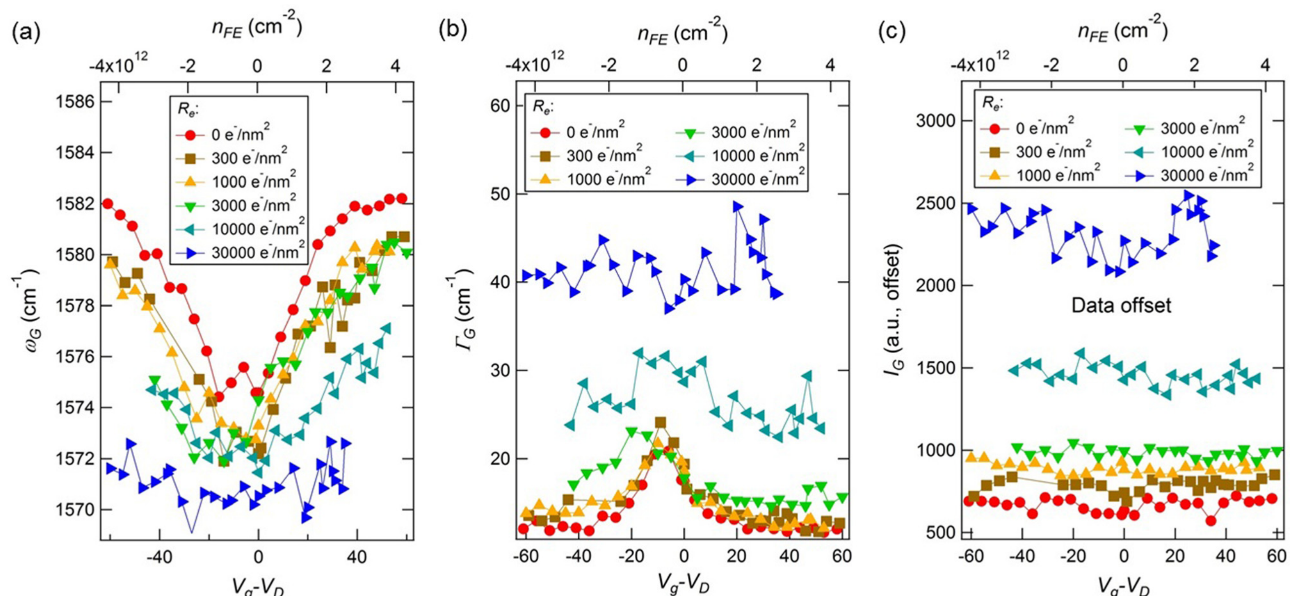

FIG. 2. Raman G peak frequency ((a), ω_G), FWHM ((b), Γ_G), and integrated intensity ((c), I_G) plotted against the gate voltage relative to the Dirac point, V_g-V_D (proportional to the carrier density, plotted on the top axis), for different dosages, R_e, of irradiation. In (c), the data sets for $R_e > 0$ e$^-$/nm^2 are offset consecutively by 100 vertically for clarity.

[This article is copyrighted as indicated in the article. Reuse of AIP content is subject to the terms at: http://scitation.aip.org/termsconditions. Downloaded to] IP: 128.210.68.204 On: Tue, 23 Dec 2014 22:27:15

at V_g ranging from −40 to +60 V away from the CNP. Again we see a trend of decreased ω_G and increased Γ_G as V_g approaches the CNP. These trends can be seen more clearly in Fig. 2. We also note that the field-effect measurements show a trend of decreasing carrier mobility and minimum conductivity as irradiation increases, which is consistent with our previous report.[16]

Fig. 2 shows the extracted ω_G (a), Γ_G (b), and G peak intensity (I_G, c) as a function of V_g–V_D, which is proportional to n_{FE} (top axis). In addition to a minimum in ω_G near the CNP for low- to medium-levels of irradiation, we also see a peak in Γ_G near the CNP for the same range of irradiation. However I_G shows no significant dependence on n_{FE} from $-4 \times 10^{12}\,\mathrm{cm}^{-2}$ to $4 \times 10^{12}\,\mathrm{cm}^{-2}$ for a fixed R_e, nor on irradiation up to $R_e = 3000$ e$^-$/nm^2. For higher R_e, the G peak becomes significantly wider and the overall intensity increases. In addition, at these high irradiation dosages ($R_e = 30\,000$ e$^-$/nm^2 and $70\,000$ e$^-$/nm^2), ω_G and Γ_G show very weak dependence on n_{FE} within the resolution of the experiment.

We note that the maxima and minima in Fig. 2 do not occur exactly at the CNP, but at some smaller V_g. Similar features can also be seen in other figures. We believe this is due to the effects of local, laser-induced doping.[24] We also note the extracted Raman parameters can show fluctuation (nonrepeatable) at larger R_e, where we expect more spatial inhomogeneity of n_{FE} due to charge puddles caused by irradiation. The fluctuation may be caused by small variations in the location of the Raman laser spot, which can be caused by small variations in the temperature in the cryostat.

Next, we look at the effect of n_{FE} on the Raman 2D peak for different R_e. We see no clear dependence of the 2D FWHM (Γ_{2D}) on n_{FE}, however the 2D peak frequency (ω_{2D}) has a broad, weak minimum near the CNP at low irradiation dosages. In Fig. 3(c), we see a maximum I_{2D} near the CNP up to $R_e = 3000$ e$^-$/nm^2. We also see a decrease in the

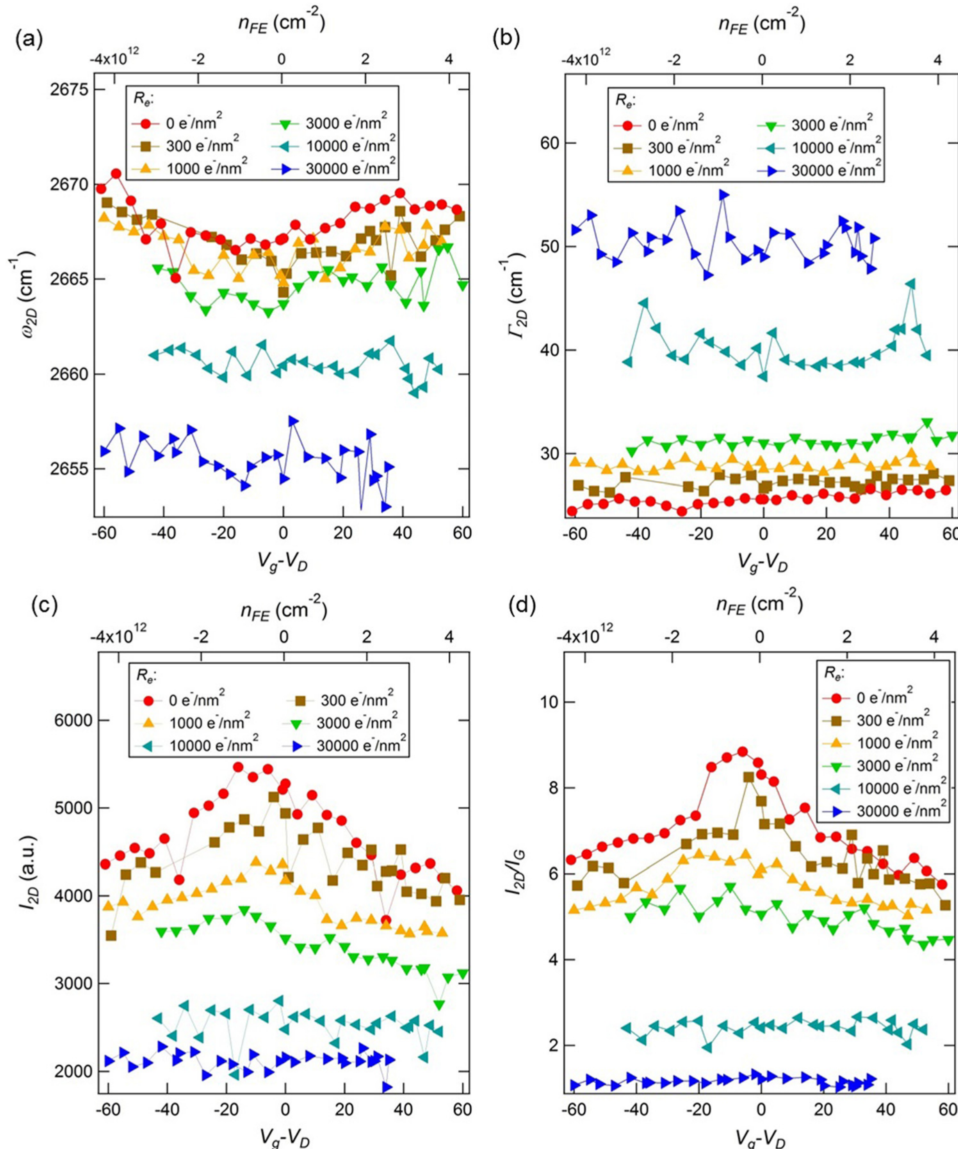

FIG. 3. Raman 2D peak frequency ((a), ω_{2D}), FWHM ((b), Γ_{2D}), integrated intensity ((c), I_{2D}), and intensity ratio ((d), I_{2D}/I_G) plotted against the gate voltage shift relative to the Dirac point, V_g-V_D (proportional to the carrier density, plotted on the top axis), for different dosages, R_e, of irradiation.

[This article is copyrighted as indicated in the article. Reuse of AIP content is subject to the terms at: http://scitation.aip.org/termsconditions. Downloaded to] IP: 128.210.68.204 On: Tue, 23 Dec 2014 22:27:15

overall intensity of the 2D peak with increasing irradiation. Due to the maximum in I_{2D} near the CNP, when we plot the ratio of the 2D and G peak intensities (I_{2D}/I_G) as a function of V_g (Fig. 3(d)), we see a clear maximum of I_{2D}/I_G near the CNP for irradiation dosages up to $R_e = 1000$ e$^-$/nm^2. I_{2D}/I_G decreases with increased irradiation, and at higher irradiation dosages ($R_e = 10\,000$ e$^-$/nm^2 and $30\,000$ e$^-$/nm^2), its dependence on n_{FE} completely disappears.

Finally, we look at the effect of n_{FE} and disorder on the D peak of graphene. The D peak shows no clear dependence of peak frequency (ω_D) or FWHM (Γ_D) on carrier density as observed. In Fig. 4(c), we see a very weak, broad peak in the D peak intensity (I_D) near the CNP for $R_e = 300$ e$^-$/nm^2 and 1000 e$^-$/nm^2 as well as an increase in I_D for all n_{FE} as the irradiation dosage increases up to $R_e = 30\,000$ e$^-$/nm^2. We also plot the intensity ratio I_D/I_G in Fig. 4(d), where we can see a weak, broad peak near the CNP for $R_e = 300$ e$^-$/nm^2 and 1000 e$^-$/nm^2. Fig. 4(d) also shows a clear trend of increasing I_D/I_G with increasing irradiation up to $R_e = 10\,000$ e$^-$/nm^2, which is expected.

From Figs. 2–4, we also note an overall decrease in the frequency and an increase in the FWHM for the D, G, and 2D peaks with increasing R_e. This can be seen more clearly in Figs. 5(a) and 5(b), which plot the change in the D, G, and 2D peak frequency and FWHM at V_g-$V_D = 0$ from an unirradiated (G and 2D peaks) or lightly irradiated (D peak) state as a function of R_e, which we believe to be proportional to the defect density (where the proportionality constant depends on the details of the electron beam interaction with respect to the graphene, which are not known). We see clear trends of decreasing frequency and increasing FWHM for all peaks as the defect density increases (increased irradiation). Of the three peaks plotted, the 2D peak shows the largest change in frequency and FWHM and shows the strongest dependence on R_e, probably due to the fact that 2D is a double-phonon peak.[19]

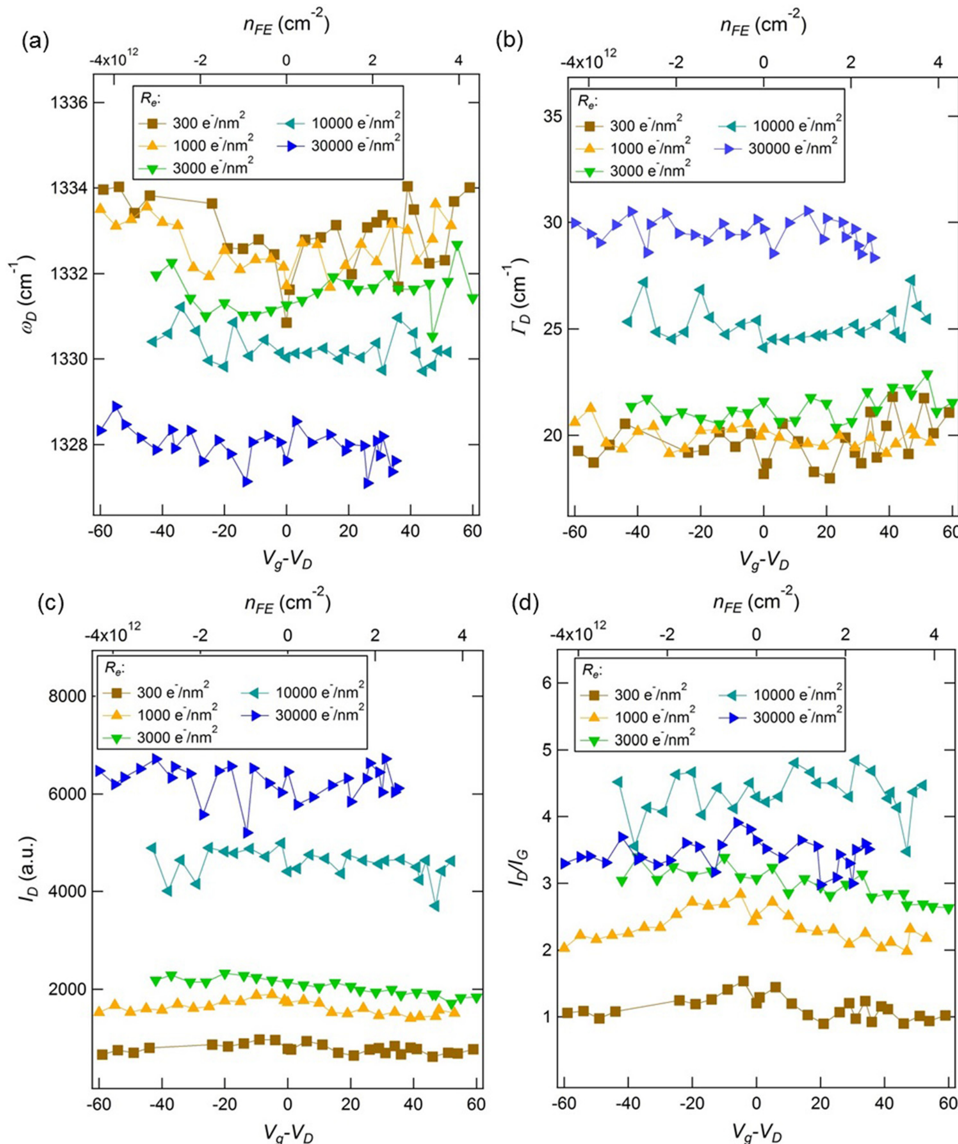

FIG. 4. Raman D peak frequency ((a), ω_D), FWHM ((b), Γ_D), integrated intensity ((c), I_D), and intensity ratio ((d), I_D/I_G) plotted against the gate voltage shift relative to the Dirac point, V_g-V_D (proportional to the carrier density, plotted on the top axis), for different dosages, R_e, of irradiation.

[This article is copyrighted as indicated in the article. Reuse of AIP content is subject to the terms at: http://scitation.aip.org/termsconditions. Downloaded to] IP: 128.210.68.204 On: Tue, 23 Dec 2014 22:27:15

ANALYSIS

The trends of increasing ω_G and decreasing Γ_G for increasing n_{FE} we see in Fig. 2 at lower R_e are similar to previous reports for pristine graphene.[8–11] These trends are attributed to the removal of the Kohn anomaly and decreased electron-phonon coupling for increased n_{FE}. Our results show that such mechanisms still exist in moderately disordered graphene. On the other hand, for $R_e < 10\,000$ e$^-$/nm^2, we observe that I_G does not vary appreciably with either R_e or n_{FE} within our measurement range.

As disorder increases (increasing R_e), ω_G and Γ_G show less dependence on n_{FE}. This could be caused by disorder dominating the phonon scattering processes, therefore reducing the effect of electron-phonon coupling. We can calculate the electron-phonon coupling strength (D) for different R_e using a linear approximation with time-dependent perturbation theory[9]

$$\hbar\omega_G - \hbar\omega_G^0 = \frac{A_{uc}D^2}{2\pi\hbar\omega_G M v_F^2}|E_F|, \quad \text{where } E_F = \hbar v_F\sqrt{\pi n_{FE}}, \tag{3}$$

$\omega_G{}^0$ is the G peak frequency at $E_F = 0$ (CNP), $A_{uc} = 0.51\,\text{nm}^2$ is the area of the graphene unit cell, $M = 2 \times 10^{-26}$ kg is the mass of a carbon atom, and $v_F = 10^6$ m/s is the Fermi velocity in graphene. This equation can be used sufficiently far away from the Dirac point where the trend of G peak energy ($E_G = \hbar\omega_G$) versus Fermi energy (E_F) is approximately linear. We perform this fitting in Fig. 5(c) (solid lines), which plots E_G versus E_F for different R_e. We plot the extracted D as a function of R_e in Fig. 5(d) (and D as a function of I_D/I_G in the inset). We see that D decreases with increasing R_e (stronger disorder with higher I_D/I_G). For the unirradiated sample, we find $D = 14.7$ ev/Å, which agrees fairly well with previous works.[9] D then decreases to $\sim$7 eV/Å for $R_e = 30\,000$ e$^-$/nm^2.

Another way to extract D, as also discussed in Ref. 9, is to use the total change in Γ_G between the CNP and sufficiently high n_{FE} (Ref. 9),

$$\Delta\Gamma = \frac{A_{uc}D^2}{8Mv_F^2}. \tag{4}$$

We also plot the extracted values of D from the data in Fig. 2(b) based on this equation as a function of R_e (except for $R_e = 30\,000$ e$^-$/nm^2 where the fluctuation in Γ_G is too large to allow such analysis) in Fig. 5(d) (and D as a function of I_D/I_G in the inset), and find the values in general agreement with D calculated from the peak frequency data (Eq. (3)), with $D = 15.3$ eV/Å for unirradiated graphene, and D decreasing for larger R_e, again suggesting that increasing disorder weakens electron-phonon coupling.

We note the possibility that increased charge inhomogeneity at larger R_e could cause a decreased dependence on V_g-induced n_{FE}. However, from our field-effect data, we conclude that the inhomogeneity is on the order of $< 2 \times 10^{12}\,\text{cm}^{-2}$ at

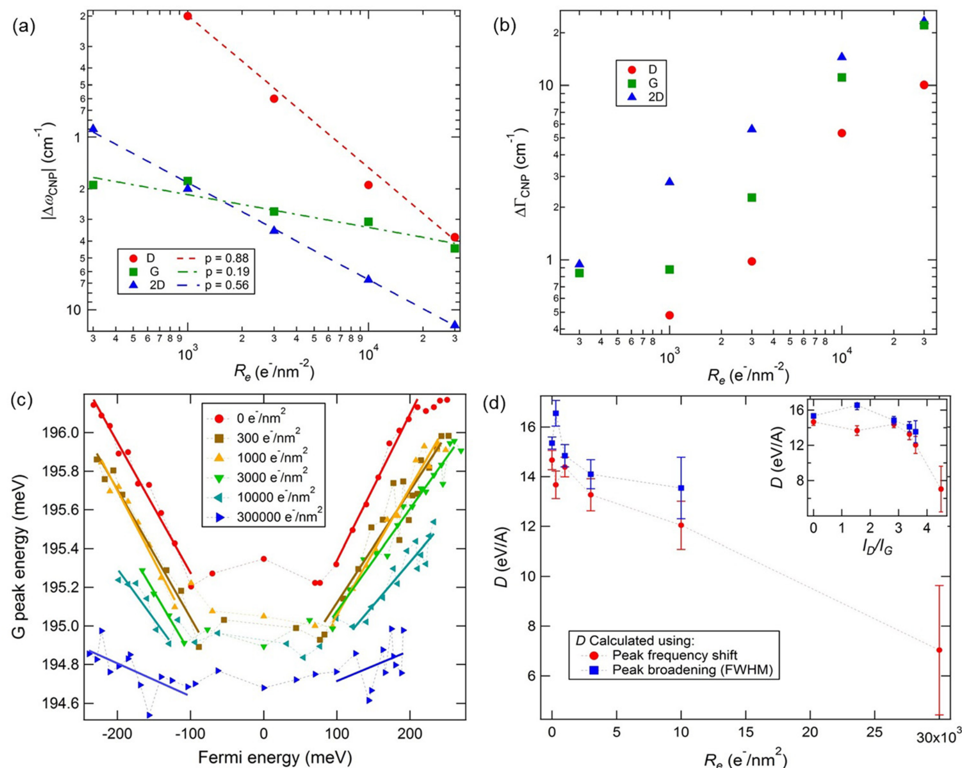

FIG. 5. The change of peak frequency, ((a), $\Delta\omega$) and FWHM, ((b), $\Delta\Gamma$) from an unirradiated state for the Raman D, G, and 2D peaks at the CNP (V-$V_D = 0$) versus the irradiation dosage, R_e, plotted in a log-log scale. The dashed lines in (a) are power law fittings to y $\propto R_e{}^p$. Since we see no significant D peak in the unirradiated state, $\Delta\omega$ and ΔFWHM for the D peak are plotted relative to $R_e = 300$ e$^-$/nm^2. (c) The energy of the Raman G peak (E_G) versus the Fermi energy (E_F) of the graphene for different dosages, R_e, of irradiation. The solid lines are linear fittings (Eq. (3)) far away from $E_F = 0$. (d) Electron-phonon coupling strength (D) versus R_e. For each R_e, D is calculated both from the measured E_F dependence of ω_G (data in c) by fitting to Eq. (3) as well as from the E_F dependence of Γ_G (broadening near CNP, from FWHM data in Fig. 2(b)) using Eq. (4).

[This article is copyrighted as indicated in the article. Reuse of AIP content is subject to the terms at: http://scitation.aip.org/termsconditions. Downloaded to] IP: 128.210.68.204 On: Tue, 23 Dec 2014 22:27:15

the highest R_e measured. This is significantly smaller than our measurement range, implying inhomogeneity alone is not the cause of the disappearance of n_{FE} dependence in ω_G and Γ_G.

We also note that Eqs. (3) and (4) are based on pristine graphene models and error may be introduced when these equations are applied to disordered graphene. In particular, at some graphene sites near "shuffle" dislocations, the local density of states is shown to have a peak at $E_F = 0$ instead of a valley.[25] This would create an error in our calculation of E_F for Eq. (3), however Eq. (4) is not dependent on E_F, so we believe our analysis is still valid.

We also see trends of decreasing peak position and increasing FWHM with increasing R_e for the G, 2D, and D peaks, which can be seen clearly in Fig. 5 and are consistent with the results in Ref. 19. We attribute the trend of decreasing frequency to a softening of the lattice caused by defects, which would reduce the energy of lattice vibrational modes. We fit the peak frequency trends to a phenomenological power law, $\Delta\omega \propto R_e^{p}$, and find power dependences of $p = 0.88$, 0.19, and 0.56 for the D, G, and 2D peaks, respectively. We can attribute the increasing FWHM to increased phonon scattering due to defects, which will decrease phonon lifetime. In fact, the FWHM can be described as a sum of contributions from phonon-phonon interactions (γ^{an}), electron-phonon interactions (γ^{EPC}),[12] and phonon defect scattering (γ^{D}). We have demonstrated a decrease in γ^{EPC} with increased disorder and would expect a similar decrease in γ^{an}. These reduced interactions would reduce the peak FWHM, so an increased FWHM with increased disorder must be caused by increased γ^{D}. One other trend to note is that Γ_G remains relatively constant for low levels of disorder, which is consistent with previous results.[26]

The 2D and D peak frequencies and widths do not have a significant dependence on n_{FE}, however their integrated intensities show some dependence on n_{FE} at $R_e < 3000$ e$^-$/nm^2. At these dosages, both I_{2D} and I_D decrease with increased n_{FE}. For the 2D peak, this dependence has been previously studied in pristine graphene and the intensity ratio I_{2D}/I_G cited as an important parameter to estimate doping concentration[10] (in addition, I_{2D}/I_G is commonly used to determine the number of layers in graphene),[27] however, we note that attention should also be paid to the disorder level, as increased R_e causes a weakening of I_{2D}/I_G's dependence on n_{FE} and an overall decrease in its value. In addition, the strong dependence of I_D on disorder has been used to characterize L_D in terms of the intensity ratio I_D/I_G.[13–18] At low values of irradiation, however, we show this ratio also has a weak dependence on n_{FE}, and this dependence has not been captured in previous models of L_D with respect to I_D/I_G.

We have demonstrated that both disorder and n_{FE} affect a number of Raman peak parameters, including peak position, width, and intensity for the D, G, and 2D modes. We measured these effects and have concluded that increased n_{FE} in graphene increases phonon energy and decreases phonon scattering, while increased disorder reduces electron-phonon coupling and increases phonon scattering. Our results are valuable for understanding Raman spectra and electron-phonon physics in doped and disordered graphene, and they suggest attention should be paid to both disorder and carrier density when characterizing graphene through Raman spectra.

[1]H. Raza, Graphene Nanoelectronics: Metrology, Synthesis, Properties and Applications (Springer, Berlin, 2012).
[2]A. K. Geim and K. S. Novoselov, Nat. Mater. **6**, 183 (2007).
[3]R. Saito, M. Hofmann, G. Dresselhaus, A. Jorio, and M. S. Dresselhaus, Adv. Phys. **60**, 413 (2011).
[4]A. C. Ferrari and D. M. Basko, Nat. Nanotechnol. **8**, 235 (2013).
[5]I. Childres, L. A. Jauregui, W. Park, H. Cao, and Y. P. Chen, in *New Developments in Photon and Materials Research*, edited by. J. I. Jang (Nova Science Publishers, 2013), Chap. 19.
[6]A. C. Ferrari, J. C. Meyer, V. Scardaci, C. Casiraghi, M. Lazzeri, F. Mauri, S. Piscanec, D. Jiang, K. S. Novoselov, S. Roth, and A. K. Geim, Phys. Rev. Lett. **97**, 187401 (2006).
[7]S. Piscanec, M. Lazzeri, A. C. Ferrari, F. Mauri, and J. Robertson, in *2004 MRS Fall Meeting – Functional Carbon Nanotubes*, edited by D. L. Carroll, B. Weisman, S. Roth, and A. Rubio (Mater. Res. Soc. Symp. Proc., 2005), Vol. 858E, p. HH7.4.1.
[8]S. Pisana, M. Lazzeri, C. Casiraghi, K. S. Novoselov, A. K. Geim, A. C. Ferrari, and F. Mauri, Nat. Mater. **6**, 198 (2007).
[9]J. Yan, Y. Zhang, P. Kim, and A. Pinczuk, Phys. Rev. Lett. **98**, 166802 (2007).
[10]A. Das, S. Pisana, B. Chakraborty, S. Piscanec, S. K. Saha, U. V. Waghmare, K. S. Novoselov, H. R. Krishnamurthy, A. K. Geim, A. C. Ferrari, and A. K. Sood, Nat. Nanotechnol. **3**, 210 (2008).
[11]A. Das, B. Chakraborty, and A. K. Sood, Mod. Phys. Lett. B **25**, 511 (2011).
[12]A. C. Ferrari, Solid State Commun. **143**, 47 (2007).
[13]F. Tuinstra and J. L. Koenig, J. Chem. Phys. **53**, 1126 (1970).
[14]D. Teweldebrhan and A. A. Balandin, Appl. Phys. Lett. **94**, 013101 (2009).
[15]M. M. Lucchese, F. Stavale, E. H. Ferreira, C. Vilani, M. V. O. Moutinho, R. B. Capaz, C. A. Achete, and A. Jorio, Carbon **48**, 1592 (2010).
[16]I. Childres, L. A. Jauregui, M. Foxe, J. Tian, R. Jalilian, I. Jovanovic, and Y. P. Chen, Appl. Phys. Lett. **97**, 173109 (2010).
[17]I. Childres, L. A. Jauregui, J. Tian, and Y. P. Chen, New J. Phys. **13**, 025008 (2011).
[18]L. G. Cancado, K. Takai, and T. Enoki, Appl. Phys. Lett. **88**, 163106 (2006).
[19]E. H. M. Ferreira, M. V. O. Moutinho, F. Stavale, M. M. Lucchese, R. B. Capaz, C. A. Achete, and A. Jorio, Phys. Rev. B **82**, 125429 (2010).
[20]G. Rao, S. Mctaggart, J. U. Lee, and R. Geer, in *2009 MRS Spring Meeting - Electron Crystallography for Materials Research and Quantitive Characterization of Nanostructured Materials*, edited by P. Moeck, S. Hovmoller, S. Nicolopoulos, S. Rouvimov, V. Petkov, M. Gateshki, and P. Fraundorf (Mater. Res. Soc. Symp. Proc., 2009) Vol. 1184, p. HH03-07.
[21]P. Blake, E. W. Hill, A. H. Castro Neto, K. S. Novoselov, D. Jiang, R. Yang, T. J. Booth, and A. K. Geim, Appl. Phys. Lett. **91**, 063124 (2007).
[22]B. W. Smith and D. E Luzzi, J. Appl. Phys. **90**, 3509 (2001).
[23]A. Carpio and L. L. Bonilla, Phys. Rev. B **78**, 085406 (2008).
[24]A. Tiberj, M. Rubio-Roy, M. Paillet, J.-R. Huntzinger, P. Landois, M. Mikolasek, S. Contreras, J.-L. Sauvajol, E. Dujardin, and A.-A. Zahab, Sci. Rep. **3**, 2355 (2013).
[25]A. Carpio, L. L. Bonilla, F. de Juan, and M. A. H. Vozmediano, New J. Phys. **10**, 053021 (2008).
[26]L. G. Cancado, A. Jorio, E. H. M. Ferreira, F. Stavale, C. A. Achete, R. B. Capaz, M. V. O. Moutinho, A. Lombardo, T. S. Kulmala, and A. C. Ferrari, Nano. Lett. **11**, 3190 (2011).
[27]A. Gupta, G. Chen, P. Joshi, S. Tadigadapa, and P. C. Eklund, Nano Lett. **6**, 2667 (2006).

[This article is copyrighted as indicated in the article. Reuse of AIP content is subject to the terms at: http://scitation.aip.org/termsconditions. Downloaded to] IP: 128.210.68.204 On: Tue, 23 Dec 2014 22:27:15